Penalty-Aware Bidding for Virtual Power Plants: A Robust Integration of Penalty Regimes

Nicolò Toia[a], Matteo Badialetti[a], Francesca Orlando[b], Giacomo Olivero[b], Riccardo Ramaschi[a], Julien Rappe[c], Vinicio Lupo[c], Sonia Leva[a], Tania Cerquitelli[b]

[a]*Department of Energy, Politecnico di Milano, Milan, Italy*
[b]*Department of Control and Computer Engineering, Politecnico di Torino, Turin, Italy*
[c]*Free2move eSolutions S.p.A., Milan, Italy*

Abstract

As Electric Vehicle (EV) aggregators assume a growing role in ancillary services markets, they face the dual challenge of meeting strict reliability requirements while mitigating financial penalties for shortfalls. This paper presents a penalty-aware flexibility bidding model that explicitly integrates potential penalty costs for reserve shortfalls into the aggregator's bidding objective function, effectively internalizing reliability risk as a cost factor. The penalty integration is performed by a completely generalisable formulation, where the penalties' growth rate is the core of the analysis. The proposed approach is benchmarked against two baseline strategies that do not internalize penalty costs: an analytical Extreme Value Theory-based reliability optimization method and a sample-based Mixed-Integer Linear Programming approach. Simulations on real-world EV fleet data show that the penalty-aware model yields higher net revenues than both baseline strategies. At the same time, it maintains near-optimal reliability under realistic penalty regimes. Overall, this approach enables EV aggregators to capture greater value from flexibility markets with minimal compromise in reliability.

Keywords: Ancillary Services, Electric Vehicles, Flexibility Markets, Reliability, Stochastic Optimization, Penalties

1. Introduction

The transformation of power systems across Europe is being driven by the combined effect of decarbonization, decentralization and digitalization [1]. As

renewable energy sources are becoming more widespread, the need for system operators of new flexibility forms that can balance supply and demand in real time has increased. In this context, Virtual Power Plants (VPPs) have emerged as an essential platform for integrating and coordinating heterogeneous Distributed Energy Resources (DERs), including photovoltaic generation, battery energy storage systems, industrial demand response and, more recently, Electric Vehicles (EVs) [2]. VPPs act as aggregators, enabling assets that would otherwise be too small or too volatile to participate in electricity markets to be controlled and dispatched collectively [3]. Coupling of EV flexibility with other flexibility-provider technologies is studied in [4], where the authors developed a design structure matrix to assess the system-wide impacts, integration risks, and readiness of emerging grid technologies. These platforms make it possible to aggregate flexibility from across the grid and offer it as a unified service, effectively replicating the role of a traditional power plant in terms of market behavior and grid support [5].

Among the diverse applications of VPPs, one of the most promising developments is the integration of EVs through Vehicle-to-Grid (V2G) technologies [6]. By enabling bidirectional energy flows, V2G allows EVs to adjust their charging patterns and to discharge stored energy back into the grid when needed. This transforms parked EVs from passive loads into active contributors of flexibility [7]. When aggregated within a VPP, fleets of EVs represent a highly responsive and geographically distributed resource capable of providing ancillary services [8]. Nonetheless, state-level incentives for EV adoption and VPP participation are crucial to foster system-level benefits [9]. Moreover, the integration of EVs into VPPs also presents new operational challenges, as stochasticity, user-dependency of EV availability [10], and context-specific limitations [11]. This highlight on one hand the need of novel methods for aggregating flexibility from EVs [12, 13, 14], and, on the other hand to carefully design market strategies that can manage risk while exploiting value of flexibility, in order to find a balance between reliability and profitability. This issue becomes even more relevant under new regulatory regimes, such as the Italian TIDE framework [15], which formally recognize aggregators as market actors and introduce shorter market intervals and strict performance-based penalties.

To address this challenge and take advantage of emerging opportunities in this evolving landscape, this work focuses on optimal bidding strategy for a VPP composed of EVs, with a focus on participation in ancillary services markets, aligned with EVs operational constraints, which consist of short and

high-speed flexibility rather than long-duration energy delivery [16].

In scientific literature, the majority of studies addressing the participation of stochastic resources in ancillary service markets assume perfect availability without deeply considering market penalties [17, 18]. Various contributions treat reliability as a hard constraint and evaluate penalties only ex post [19], rather than incorporating them directly into the bidding optimization. Existing bidding strategies for aggregators typically incorporate simplified penalty cost models [20], often assuming static [21] or linear formulations [22, 23]. When more complex penalty mechanism are introduced [24, 25], authors still overlook the penalty growth rate and focus on market-specific shapes, reducing the model robustness. To bridge this gap, this study aims to explicitly incorporate the risk of non-performance into the bidding process by modelling penalty growth rate directly in the objective function. The proposed generalisable penalty formulation constitutes the main novelty of this work with respect to the existing literature. To our knowledge, the state of the art work regarding EV-based VPP participation in ancillary services is [26] by Herstad *et al.*, which constitutes the starting point of this work for what concerns the optimization framework. The strategy models the uncertain availability of EVs using a chance-constrained formulation and generates reliable bids based on tail-risk quantification. However, financial penalties associated with deviations are not embedded in the bidding objective neither considered in post-analysis. A related contribution is the work by Lunde *et al.* [27] which also adopts a probabilistic approach to bidding under uncertainty, based on real-world data from a large EV fleet. While their model ensures a high reliability level in reserve provision, the cost of under-delivery is not included in the bidding objective. Instead, penalties are computed ex post as part of the performance evaluation, without influencing the actual bidding decisions. By contrast, the approach proposed in this paper embeds expected penalty regimes directly into the optimization problem. This allows the aggregator to balance profitability and reliability in a unified framework, adapting bids according to the severity of the penalty regime rather than enforcing fixed reliability thresholds. Moreover, out of scope of this article but still relevant to frame our work, this reliability-oriented bidding strategy can be seen as an input to an intelligent scheduling managing the system operation perspective [28].

In order to frame this contribution, the paper is structured as follows. Section 2 reviews the current participation of VPP operators in European electricity markets and outlines the main aspects of the Italian TIDE frame-

work. Together, these elements establish the regulatory and operational context for the proposed bidding strategy. The problem is formulated in Section 3, introducing two baseline bidding approaches, the proposed penalty regime generalization and the used metrics for carrying out the analysis. Our penalty-aware model is outlined in Section 4, focusing on its formulation and on the contribution with respect to the baseline models. The case study is presented in Section 5, from the employed EV fleet database description to the obtained results in terms of several metrics. Finally, Section 6 summarises the key findings and outlines future research directions.

2. Virtual Power Plants in Flexibility Markets: strategic benchmark and Italian Regulatory Framework

Recently, the role of VPPs in electricity markets has moved well beyond the pilot stage. Across Europe, energy and technology companies are actively expanding their aggregation capabilities and aligning their business strategies with the growing demand for grid flexibility [29]. VPPs are increasingly seen not only as technical platforms for resource coordination, but as commercial actors offering market-driven services across multiple domains. In particular, companies are focusing on the integration of DERs with the goal of participating in wholesale energy markets and, more prominently, in ancillary services markets [29, 30].

A clear trend among market operators is the pursuit of multi-market participation models: VPPs are designed to operate flexibly across day-ahead and intraday markets, while also bidding into balancing and reserve service mechanisms [31]. In many European countries the most commercially viable focus is on ancillary services such as Frequency Containment Reserve (FCR), automatic Frequency Restoration Reserve (aFRR) and manual Frequency Restoration Reserve (mFRR). Market players are also exploring synergies with demand response and EV charging infrastructures to enhance the temporal and spatial granularity of the flexibility they can offer [32]. From the said synergies, [33] identified benefits and vulnerabilities of integrating growing EV fleets in aggregating entities. As noted in [34], EV integration in distribution networks calls for significant adaptations or new solutions once penetration levels exceed 50%. One such approach is proposed by [35], who incorporate EV-induced uncertainty into a system resilience optimization framework. In Italy, alongside developments at the national level, interest in the creation of local flexibility platforms by Distribution System Operators

(DSOs) is increasing. For instance, Free2move eSolutions [36], a mobility and energy services provider, is investigating EV-based VPP participation in flexibility provision. Several pilot initiatives have tested the ability of VPPs to offer location-specific services such as congestion management and voltage regulation in urban networks [37]. These pilots mirror a broader shift in system architecture, from centralized dispatching to decentralized and market-based coordination, and signal a regulatory openness to new actors capable of providing fast and distributed responses. The Italian market is thus evolving in parallel with broader European trends, where regulatory adjustments, digital infrastructure and commercial interest are converging to make VPPs a standard feature of electricity markets.

Taken together, these elements demonstrate that companies across Europe are positioning VPPs as strategic tools for participating in flexibility markets. Rather than operating solely as technology integrators, aggregators are actively building business models around energy market participation. This context motivates the present work, which aims to define a strategy for VPP participation that reflects both current market structures and operational risks.

The regulatory landscape plays a defining role in shaping the participation of new actors in electricity markets. In Italy, the implementation of the TIDE (Testo Integrato del Dispacciamento Elettrico) in January 2025 marks a fundamental step toward a more flexible, efficient and inclusive energy system [15]. Developed by ARERA and implemented by the TSO, Terna, TIDE makes Italy aligned with European directives [38] and addresses the structural need for integrating distributed flexibility in a high-renewable grid. It introduces various technical and market innovations that modernize market mechanisms and also create tangible new opportunities for Virtual Power Plants to participate in balancing services, even if its complexity increases.

The main features of TIDE are:

- Shorter market intervals: Market Time Units reduced from 60 to 15 minutes, increasing granularity in energy balancing and enabling short duration assets (EVs batteries) to partecipate more effectively.

- Zonal balancing prices: replacement of the Uniform National price with zonal pricing, reflecting local grid constraints and increasing locational efficiency and the value of flexibility in congested areas, where EVs batteries can deliver high-impact services.

- Definition of market roles: separation of Balancing Service Provider (BSP) and Balance Responsible Party (BRP) roles. VPPs can act as BSPs, aggregating and offering flexibility without managing directly energy portfolio imbalances.

The formal recognition of aggregators as market entities with defined rights and obligations under TIDE reflects a broader shift toward a more distributed and participatory market model. However, with this recognition come strict performance requirements: being formally market entities, BSPs are required to deliver contracted services within strict performance tolerances. Deviations from schedule, whether due to over-delivery or under-delivery, can lead to financial penalties and imbalance settlements.

These regulatory provisions are designed to ensure system reliability but also introduce significant strategic complexity for VPPs managing EVs, flexible but uncertain resources. For instance, if a VPP composed of EVs bids a certain quantity of upward reserve based on statistical forecasts of vehicle behavior, but less is available at dispatch time, the aggregator may be liable for imbalance charges or face contractual penalties. This risk becomes more pronounced as market intervals shorten and activation frequencies increase, demanding precise control and accurate real-time forecasting of available flexibility [39].

Consequently, participation under TIDE requires not only technical capability but also advanced forecasting, risk assessment and bidding strategies that can hedge against performance uncertainty while maintaining economic viability [40]. For EV-based VPPs, this involves the integration of behavioral models, battery state-of-charge forecasts and probabilistic availability profiles into their market algorithms. Moreover, because ancillary service revenues can be entirely offset by non-performance penalties, sanctions imposed when energy or flexibility committed in a market bid is not delivered as contracted, bidding strategies must incorporate explicitly market risks and align offers with statistically reliable flexibility reserves. Only by combining operational intelligence and market optimization VPPs operators can sustainably capture the new revenue opportunities enabled by TIDE [41].

In sum, TIDE represents both an enabler and challenge for VPPs in Italy. It creates a more open and locationally responsive market, well suited to flexible assets like EVs, while imposing stricter reliability requirements. Exploring this duality is central to the strategic evolution of VPP operators and lies at the core of the optimization framework proposed in this study.

Notably, the EDGE project, initiated by the Italian DSO E-Distribuzione, exemplifies this approach by piloting local flexibility markets that aggregate resources such as EV batteries, storage systems and distributed generation to provide ancillary services, thereby enhancing grid resilience and supporting the integration of renewable energy sources [42].

3. Problem Formulation and State of the Art Implementation

Building on the framework proposed by [26], we tailor the EV-based VPP bidding strategy to the Italian context in accordance with the TIDE regulation. To ensure broader applicability, we further develop a generalized formulation that abstracts market-specific rules (e.g. product structure, performance obligations, and penalty mechanisms) into explicit, parametric components, allowing the model to be instantiated across different regulatory regimes and study designs. While preserving the core modelling principles of the original approach, our adaptations allow the consideration of heterogeneous operational scenarios, thereby enhancing the robustness and reliability of the resulting bidding strategy. Our methodology is founded upon a joint chance-constrained optimization model, extending the frameworks proposed by [26] and [27]. We introduce a generalized formulation that can be adapted to diverse market regulations by parameterizing the delivery constraints:

$$\max_{b^{\downarrow}, b^{\uparrow} \geq 0} \quad b^{\uparrow} + b^{\downarrow}$$

subject to:

$$\mathbb{P}\left(\begin{array}{c} \alpha b^{\downarrow} + b^{\uparrow} \leq R^{\uparrow} \\ \beta b^{\uparrow} + b^{\downarrow} \leq R^{\downarrow} \\ max(\gamma b^{\downarrow}, \delta b^{\uparrow}) \leq R^{E,T} \end{array} \right) \geq 1 - \varepsilon$$

The objective function maximizes the total offered capacity by summing the upward ($b^{\uparrow}$) and downward ($b^{\downarrow}$) bids. The joint chance constraint ensures that the offered bids are deliverable with a predefined reliability level of $1-\varepsilon$, where $R^{\uparrow}$, $R^{\downarrow}$, and $R^{E,T}$ represent the stochastic available upward flexibility, downward flexibility, and energy, respectively. The dimensionless parameters α, β, γ and δ provide the flexibility to model specific regulatory requirements, such as the coupling between upward and downward reserve provision. In our case study, which is aligned with the Italian TIDE framework, we set the coupling constants α and β to zero, as the upward and downward services are considered uncoupled. Furthermore, the parameters γ and δ are set to unity

($\gamma = \delta = 1$). This specific configuration is adopted for scenarios involving participation with bi-directionally energy-limited resources, such as Vehicle-to-Grid (V2G) batteries, which require deliverability for 15 minutes in both upward and downward directions. This implies that the same energy budget is used for both directions, leading to the constraint $\max\{b^{\uparrow}, b^{\downarrow}\} \leq R^{E,15}$, in alignment with the TIDE framework. The violation probability ε is set to 0.1, in accordance with the common requirement for ancillary services of 90% reliability [26]. To avoid spurious small bids, we implemented a minimum bid threshold, reflecting common aggregator practice.

3.1. Analytical Approach (EVT-Based Reliability Model)

A first baseline follows the chance-constrained strategy proposed by Herstad *et al.* [26]. In the Nordic FCR-D context, the aggregator must ensure at least 90 % probability that it can deliver its promised capacity; we can assume the same scenario is valid for the Italian and European market. Formally, if $A_h^{\uparrow}$ and $A_h^{\downarrow}$ denote the random available upward and downward flexibility in a given hour h, the reliability requirement can be stated as the joint chance constraint

$$\mathbb{P}\Big(A_h^{\uparrow} \geq b_h^{\uparrow},\ A_h^{\downarrow} \geq b_h^{\downarrow},\ A_h^{E} \geq \text{energy}\big(b_h^{\uparrow}, b_h^{\downarrow}\big)\Big) \ \geq\ 90\% \tag{1}$$

Here $b_h^{\uparrow}$ and $b_h^{\downarrow}$ are the upward and downward capacity bids for hour h, and A_h^{E} is the available battery energy for that hour (which limits the response duration). Directly enforcing this joint probability is intractable, so the analytical approach uses a conservative Bonferroni approximation. The idea is to control each delivery constraint's failure probability at $\delta/3$ (with $\delta = 10\%$ for 90 % overall reliability) so that *any* violation remains below 10 % by the union bound. In practice, each bid is therefore chosen as an extreme quantile of the respective availability distribution.

The model leverages Extreme Value Theory (EVT) to extrapolate these quantiles. Specifically, for every hour h, a Weibull distribution is fitted to the lower tail (the worst 10%) of observed flexibility (upward, downward and energy) in the training set. The Weibull distribution was selected based on a diagnostic comparison with the Generalized Pareto Distribution and Generalized Extreme Value distribution. Goodness-of-fit tests were employed to statistically measure how well the chosen distribution matches the empirical data. The results confirmed the suitability of the Weibull model, which passed the Kolmogorov-Smirnov test for all 24 hours with a high mean p-value

of 0.801. Full details of the goodness-of-fit analysis and model selection are reported in Appendix A.

Let $F_h^{\uparrow}(x)$ denote the fitted CDF of upward availability; the upward bid is then the $(\delta/3)$-quantile,

$$b_h^{\uparrow} \;=\; \inf\bigl\{x \;:\; F_h^{\uparrow}(x) \;\geq\; \delta/3\bigr\}, \tag{2}$$

and $b_h^{\downarrow}$ is obtained analogously (as is any energy-constrained combination of up/down).

This construction yields a robust offer that *statistically* caps the non-delivery risk for each constraint at approximately 3.3%, ensuring the overall default probability is $\approx$ 10% or lower. By concentrating on the extreme lower tail of flexibility, the EVT-based method explicitly accounts for rare low-availability events that could cause under-delivery. The result is a transparent, analytical bidding rule that balances revenue with high reliability. Notably, Herstad *et al.* [26] reports that this EVT approach outperforms a conventional scenario-based optimization in out-of-sample violation rates, underscoring the value of a rigorous statistical treatment of extreme cases.

3.2. Sample-Based Approach (Chance-Constrained MILP)

Authors in [26] proposed as a benchmark *sample-based chance-constrained optimization*, which directly determines bids from historical (or synthetic) samples of available flexibility. The problem is formulated as a Mixed-Integer Linear Program (MILP) that maximises the aggregator's offered capacity while capping the fraction of scenarios with delivery shortfalls. For each hour h, let $\omega = 1, \ldots, N$ index the training scenarios of availability $(A_{h\omega}^{\uparrow}, A_{h\omega}^{\downarrow}, A_{h\omega}^{E})$. Decision variables $b_h^{\uparrow}, b_h^{\downarrow} \geq 0$ represent the bids, and binary slack variables $z_{h\omega} \in \{0, 1\}$ indicate whether scenario ω is allowed to violate delivery constraints. The MILP is:

Objective: maximise total offered flexibility,

$$\max\,(b_h^{\uparrow} + b_h^{\downarrow}),$$

or equivalently expected revenue, since each kW offered is paid.

Delivery constraints: for every scenario ω enforce

$$b_h^{\uparrow} \leq A_{h\omega}^{\uparrow} + M\, z_{h\omega}, \tag{3}$$

$$b_h^{\downarrow} \leq A_{h\omega}^{\downarrow} + M\, z_{h\omega}, \tag{4}$$

$$b_h^{E} \leq A_{h\omega}^{E} + M\, z_{h\omega}, \tag{5}$$

where M is a large constant. If $z_{h\omega} = 0$, all constraints must hold (no violation in scenario ω); if $z_{h\omega} = 1$, scenario ω may violate one or more constraints (big-M relaxation).

Chance constraint: $\sum_{\omega=1}^{N} z_{h\omega} \leq \lfloor \rho N \rfloor$,

where ρ is the tolerated violation rate (e.g. $\rho = 10\%$ for 90 % reliability). Thus at most 10 % of scenarios may exhibit any shortfall.

Solving this MILP yields bids $b_h^{\uparrow}$ and $b_h^{\downarrow}$ that *maximise capacity* while ensuring at least 90 % of historical scenarios have no violations. The optimiser pushes bids as high as possible but not so high that more than 10 % of training outcomes would fall short. This data-driven approach implicitly leverages the empirical distribution of flexibility, providing a risk-aware strategy that balances revenue and reliability. However, it produces a mixed-integer problem that can be computationally heavy, and it treats the 90 % reliability threshold as a hard cut-off (any additional risk beyond 10 % is forbidden rather than traded off against reward).

3.3. Metrics and Penalty introduction

Both baseline models are trained on 60 % of the available data (training set) and their performance is evaluated on the remaining 40 % (test set) to assess out-of-sample reliability. To compare strategies, we compute the violation rate, penalty costs, and other metrics. The violation rate is defined as the percentage of test scenarios in which any reliability constraint is violated beyond a small tolerance, to avoid numerical approximations. This essentially measures how often an approach would fail to deliver its promised energy in real operation.

Additionally, to evaluate how each strategy performs under different market conditions, we designed a specific penalty configuration involving three distinct penalty topologies: linear, quadratic, and exponential. Rather than focusing on a single functional shape, we analysed how the growth rate of penalties affects bidding behaviour, aiming to design bidding strategies that remain robust under different market conditions.

The shortfall Δ is defined as the absolute difference between the bid and the delivered energy:

$$\Delta = |\text{bidded energy} - \text{provided energy}|$$

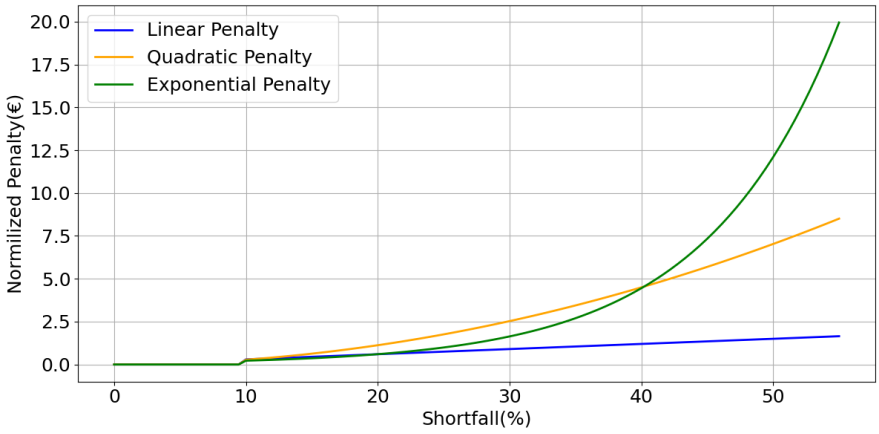

Figure 1: Example of penalty calibration for $SF = 2$ versus shortfall intensity.

Consistent with the adopted reliability requirement, a 10% tolerance is permitted, meaning no penalties are applied for shortfalls below this threshold. This provides a small margin for error. For shortfalls exceeding 10%, the penalties are defined by the following parametric forms, where $\Delta_{\%}$ represents the shortfall percentage and SF is a parameter to adjust the overall penalty strength (scale factor):

$$\begin{aligned} \text{Linear:} \quad & \text{penalty} = \left(\frac{3}{2} \cdot \Delta_{\%}\right) \cdot SF \\ \text{Quadratic:} \quad & \text{penalty} = \left(\left(\frac{15}{4} \cdot \Delta_{\%}\right)^2\right) \cdot SF \\ \text{Exponential:} \quad & \text{penalty} = \left(e^{10 \cdot \Delta_{\%} - \frac{16}{5}}\right) \cdot SF \end{aligned} \tag{6}$$

These specific formulations were constructed to model distinct market scenarios. As illustrated in Figure 1, the three penalty shapes are calibrated to start at a similar point just above the 10% shortfall threshold, with the exponential penalty being slightly lower initially.

The rationale for each shape from a market perspective is as follows:

- The linear penalty, where the cost is directly proportional to the magnitude of the under-delivery.
- The quadratic penalty represents a more severe market. It diverges immediately from the linear path, imposing significantly higher costs

for shortfalls, even those only moderately above the 10% limit. This shape stress-tests the strategic ability to avoid even small-to-medium sized misses.

- The exponential penalty is designed to simulate a market with catastrophic consequences for large failures. It remains below the linear penalty until a 20% shortfall and intersects the quadratic penalty at approximately 40%. Beyond this point, it "explodes", representing an extreme sanction like contract termination.

The scale factor allows for the simulation of varying market strengths. As it increases, not only does the overall penalty cost rise, but the delta between the different penalty shapes also enlarges, amplifying their distinct characteristics. A more detailed analysis of these penalty structures is provided in the Appendix B. For every strategy, we apply these penalty models to the test outcomes to compute total incurred penalties and net revenues, ensuring a fair comparison of how each bidding strategy generalizes and how sensitive it is to different penalty structures.

3.3.1. Advanced Reliability and Risk Metrics

Beyond simple violation rates and net revenues, a comprehensive evaluation of bidding strategies requires a richer set of risk indicators. To provide a multi-dimensional view of reliability and financial exposure, we introduce several advanced metrics:

- Penalty-to-Revenue Ratio (PRR): This metric measures financial efficiency by calculating the ratio of total penalties to gross revenue, expressed as a percentage. A lower PRR indicates that a strategy generates revenue with minimal associated penalty costs, whereas a high PRR suggests that the bids are too aggressive relative to the actual available flexibility.

$$\text{PRR} = \frac{\text{Total Penalty}}{\text{Gross Revenue}} \times 100\%$$

- Conditional Expected Shortfall (CES): This metric quantifies the "tail risk" of a bidding strategy. It answers the question: "When a violation occurs, how severe is it on average?" It is defined as the average magnitude of the shortfall, conditioned on a violation having occurred. A lower CES (measured in kW) is preferable, as it indicates that failures, when they happen, are less catastrophic.

- Severity-Weighted Violation Rate (SWVR): This provides a more nuanced view than a simple violation count by weighting each violation by its relative magnitude. It distinguishes between strategies with frequent minor violations and those with infrequent but severe ones. The formula is:
$$\text{SWVR} = \frac{\sum_{i \in \text{Violations}} \text{weight}(i)}{\text{Total Hours}}$$
where the weight is a function of the shortfall magnitude for violation i, in our case we simply take the sum of the shortfalls as weights.

- Risk-Adjusted Net Revenue (RANR): Inspired by the Sharpe ratio, this metric assesses the efficiency of risk-taking. It measures the net revenue earned per unit of risk, where risk is quantified by the standard deviation of hourly shortfalls. A higher RANR indicates a more efficient strategy that balances profit generation with performance stability.
$$\text{RANR} = \frac{\text{Net Revenue}}{\sigma(\text{hourly shortfalls})}$$

These advanced metrics are critical because simple violation rates and revenues can be misleading. A strategy with a low violation rate might still be undesirable if its few violations are catastrophic (high CES). Similarly, maximizing revenue without controlling for risk (low RANR) can expose an aggregator to contract termination or severe reputational damage, which is particularly relevant as many markets impose severity thresholds in addition to frequency limits.

4. A Penalty-Aware Bidding Strategy for EV-Based VPPs

This section presents the penalty-aware bidding model developed in this paper, which builds upon the chance-constrained optimization frameworks of Herstad et al. [26] and Lunde et al. [27] by explicitly incorporating delivery risk into the economic objective of the aggregator. The core idea is to *minimise expected penalty costs while maximising bidding revenues*, thereby balancing the trade-off between reliability and profitability. As mentioned above, the novelty of our approach lies primarily in the integration of the risk of non-performance into the bidding process by modelling penalty growth rate directly in the objective function. To do that, unlike traditional chance-constrained formulations that impose delivery reliability as a hard probabilistic constraint, our model internalizes the expected penalty for potential

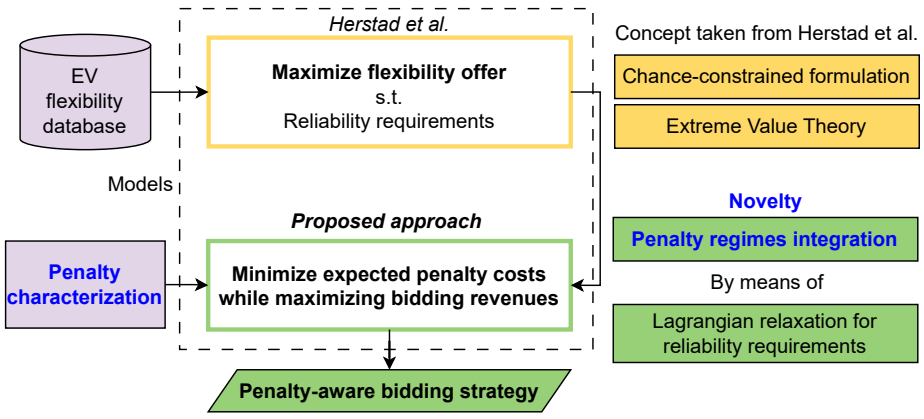

Figure 2: Methodological evolution from state-of-the-art reliability models (i.e., Herstad et al. [26]) to our penalty-aware bidding strategy. We show in blue the novelty proposition.

shortfalls directly within the objective function through a Lagrangian relaxation. A similar formulation allows controlled deviations whenever the cost of penalties is economically justified, enabling the optimization to explore a continuous trade-off between risk exposure and profit maximisation instead of enforcing a rigid compliance threshold.

Figure 2 summarizes the methodological transition from prior art to our proposed framework. The structure highlights how we build upon the chance-constrained reliability formulations of Herstad *et al.*, extending them through a Lagrangian relaxation that explicitly considers delivery penalties in the optimization process.

4.1. Optimization Model Formulation

For a given hour h, let $b_h^{\uparrow}, b_h^{\downarrow} \geq 0$ be the decision variables for upward/downward capacity to offer. We assume known energy prices $P_h^{\uparrow}$, $P_h^{\downarrow}$ for the reserve capacity (or we use a proxy like a flat tariff rate). Let $\Omega = \{\omega = 1, \ldots, N\}$ be the set of N training scenarios (drawn from the data distribution) for hour h. In each scenario ω, the available flexibility is $(A_{h\omega}^{\uparrow}, A_{h\omega}^{\downarrow}, A_{h\omega}^{E})$. The amount of available flexibility is considered in a conservative manner to account for mobility needs. Thus, SoC dynamics and intertemporal constraints - that must be considered when formulating such a problem - can be internalized in the flexibility computation, as extensively described in Section 5.1.

We first define the shortfall for each flexibility component in a given

scenario ω:

$$\Delta_{h\omega}^{\uparrow} = \max\{0,\, b_h^{\uparrow} - A_{h\omega}^{\uparrow}\}, \tag{7}$$

$$\Delta_{h\omega}^{\downarrow} = \max\{0,\, b_h^{\downarrow} - A_{h\omega}^{\downarrow}\}, \tag{8}$$

$$\Delta_{h\omega}^{E} = \max\{0,\, b_h^{E} - A_{h\omega}^{E}\}, \tag{9}$$

where these terms represent any under-delivery of upward capacity, downward capacity, and energy, respectively. The total shortfall in a scenario, $\Delta_{h\omega}^{\text{total}}$, is the sum of these components. We evaluate the shortfalls commonly as an assumption based on the EDGE project [42].

The optimization problem is formulated as a constrained non-linear program that maximizes the expected net profit. The objective function uniquely integrates a dual-penalty structure designed to control both the magnitude and the frequency of under-delivery:

$$\max_{b_h^{\uparrow}, b_h^{\downarrow} \geq 0} \quad \mathcal{R}_h - (\mathcal{P}_{\text{shortfall}} + \mathcal{P}_{\text{viol}}) \tag{10}$$

where $\mathcal{R}_h$ is the expected revenue, $\mathcal{P}_{\text{shortfall}}$ is the penalty on the magnitude of large shortfalls, and $\mathcal{P}_{\text{viol}}$ is a penalty on the overall frequency of violations.

The expected revenue term, $\mathcal{R}_h$, represents the gross income from selling the offered capacity across all scenarios:

$$\mathcal{R}_h = N \cdot (P_h^{\uparrow} b_h^{\uparrow} + P_h^{\downarrow} b_h^{\downarrow})$$

The first penalty component, $\mathcal{P}_{\text{shortfall}}$, targets the economic consequence of significant under-delivery. Crucially, this cost is conditional: it is applied only when the total shortfall in a scenario exceeds a tolerance threshold of 10% of the total bid $B_h^{\text{total}} = b_h^{\uparrow} + b_h^{\downarrow}$. The penalty is a function $f(\cdot)$ of the shortfall percentage, defined as:

$$\mathcal{P}_{\text{shortfall}} = \sum_{\omega \in \Omega} f\left(\frac{\Delta_{h\omega}^{\text{total}}}{B_h^{\text{total}}}\right) \cdot B_h^{\text{total}} \cdot \mathbb{I}(\Delta_{h\omega}^{\text{total}} > 0.1 \cdot B_h^{\text{total}})$$

Here, $\mathbb{I}(\cdot)$ is the indicator function. The shape of $f(\cdot)$ is highly adaptable; it can directly encode a known market penalty structure (e.g., linear, quadratic, exponential) or take a generic form such as $(\cdot)^p$, where the exponent p serves as a hyperparameter to infer the implicit severity of the market regime from data. In our case, $f(\cdot)$ takes the shape of the identified penalty

regimes in Eq. (6). Nonetheless, if a more general formulation - $(\cdot)^p$ - is preferred, the choice of the exponent p can be guided through cross-validation, selecting the value that best balances forecast accuracy and robustness across validation sets.

The second and most innovative component, $\mathcal{P}_{\text{viol}}$, acts as a powerful soft constraint on reliability. We first define the empirical violation rate, V_h, as the fraction of training scenarios where any shortfall occurs (i.e., $\Delta_{h\omega}^{\text{total}} > \tau$, for a small tolerance τ):

$$V_h = \frac{1}{N} \sum_{\omega \in \Omega} \mathbb{I}(\Delta_{h\omega}^{\text{total}} > \tau)$$

If this rate V_h exceeds a predefined target V_{target} (e.g., 10%), a large, quadratically increasing penalty is activated. This penalty is scaled by the base revenue to ensure it dominates the optimization, strongly guiding the solution towards reliable bids:

$$\mathcal{P}_{\text{viol}} = \mathcal{R}_h \cdot C \cdot \left(\frac{\max(0, V_h - V_{\text{target}})}{V_{\text{target}}} \right)^2$$

where C is a constant weight. This term effectively forces the optimizer to respect a desired reliability level, emulating a chance constraint without its computational rigidity. The inclusion of this penalty is crucial from both an economic and a reputational perspective. In ancillary service markets, where delivery assurance is paramount, it prevents the model from adopting a strategy of frequent, low-magnitude violations a behavior that might be profitable under lenient shortfall penalties but would be unsustainable from a market compliance and reputational standpoint.

In summary, the objective, in Eq. (10), maximizes the revenue from capacity sales minus the expected costs of shortfall and unreliability. Importantly, there are no hard delivery constraints in this formulation; instead, reliability is enforced through the two penalty terms. The optimizer is free to explore higher bids that increase revenue, but it must weigh them against the risk of incurring large shortfall penalties or a violation penalty if it over-commits. The balance struck will depend on the penalty parameters: with very high penalty weights or a very tight V_{target}, the solution tends toward a conservative bid, whereas if the penalties are set to zero, the solution trivially becomes the maximum possible bid with no regard for reliability. In this way, our soft-constraint approach generalizes prior methods by smoothly

interpolating between risk-neutral profit maximization and strict reliability compliance.

4.2. Implementation and Improvements over Baselines

We implemented the penalty-aware model using Python's optimization libraries. The dual-penalty structure, which includes conditional logic and indicator functions, renders the objective function not only non-convex but also non-differentiable. This property precludes the direct use of gradient-based optimizers, as they rely on the existence of derivatives to guide their search.

Addressing such non-differentiable problems typically involves two strategies: either smoothing the objective function to create a differentiable approximation (e.g. using sigmoid functions) or employing a derivative-free algorithm [43]. To preserve the exact formulation of the penalty structure without introducing approximations, we adopted the latter approach. Consequently, we selected the *Nelder-Mead algorithm* [44] as the optimizer, a robust direct-search method well-suited for non-differentiable problems, implemented via `scipy.optimize.minimize`.

In practice, we solve the optimization problem for each hour independently, using the corresponding training scenarios to form the objective function. The model's robustness is enhanced through several implementation details. First, non-negativity bounds are strictly enforced on the bids $b_h^{\uparrow}$ and $b_h^{\downarrow}$. Second, to stabilize the solver, the search space for each hour is constrained by pre-computed upper bounds derived from high percentiles of the training data. Finally, if the primary optimization fails to converge, we employ a multi-start fallback strategy, re-running the optimization from several conservative starting points to find a stable solution a significant improvement over defaulting to a zero bid.

The model's behavior is governed by a set of key hyperparameters that tune its response to the two penalty components.

- *Shortfall Magnitude Penalty ($\mathcal{P}_{shortfall}$)*: We calibrate the function shape $f(\cdot)$ based on domain knowledge. This reflects the common practice in ancillary service markets where penalty regimes are explicitly defined by the regulator.

- *Violation Rate Penalty ($\mathcal{P}_{viol}$)*: The key parameters are the target violation rate (V_{target}) and the scaling weight (C). We set V_{target} to 10%

to ensure a fair comparison with the baseline models, which operate under a similar reliability constraint. The weight C ensures that this goal is strictly enforced by the optimizer, in this case study $C = 1$, this allow the optimizer to find a more natural balance.

By embedding this dual-penalty mechanism, our model anticipates the long-term consequences of over-committing capacity more effectively than the baselines. It learns not just to avoid costly shortfalls but also to maintain a consistent and reliable delivery record, which is crucial for maintaining market access and reputation.

5. Numerical Results

In this section we present the numerical results obtained with the three bidding strategies on a real-world EV-fleet database, highlighting how penalty design shapes bids, reliability, and net profit.

5.1. Dataset description

For this analysis, we used a real-world database collected using telematics data, containing the anonymized travel information of 14.449 EVs from a Light Commercial Vehicle (LCV) platform during 2023. This LCV platform contains EVs with 50kWh or 75kWh battery capacity, and the data refer to business fleets, therefore we will apply our method to fleets providing flexibility in the context of delivery companies, namely in France.

Obtaining a flexibility dataset from the raw data required a thorough data preparation and pre processing. Original data contained masked information on all the charging sessions of each EV. Available (and relevant) information includes battery capacity, session-specific starting and stopping SoC, arrival and departure time, beginning and finish of the charging session. From this information, it is possible to obtain the charged energy, the charging power (as the dataset contains full-power charging sessions), and the available charging and discharging energy at the beginning of the session. The obtained charging power were clustered according to a set of typical sizes (i.e., 3, 7, 11, 22, 50, 100 and 200 kW), while if no energy exchange occurred in a session the charger size was fixed at 11 kW.

The subsequent process was the aggregation of the flexibility on a hourly basis. First of all, to ensure that the mobility needs were respected at the departure time, the sum of upward flexibility falls short of the charged energy with respect to the downward flexibility. Secondly, fraction of hours are

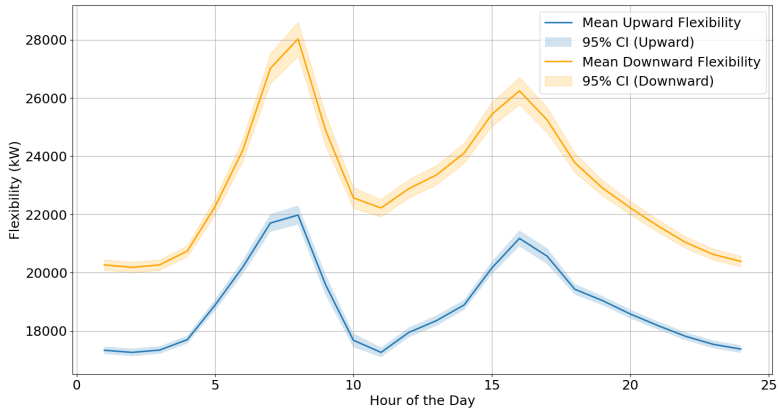

Figure 3: Upward and downward flexibility mean and 95% confidence interval: the trend shows two peaks of flexibility, one around 8 a.m. and one around 4 p.m.

accounted for while computing the available flexibility. Lastly, a balanced flexibility provision was considered to keep the EV SoC balanced, therefore the initial available charging and discharging energy were taken into account. As mentioned in the problem formulation and as described here, the flexibility computation inherently considers SoC dynamics and intertemporal constraints at the single EV level. From the practical point of view, each EV flexibility is derived conservatively to account for its mobility needs. These flexibilities are then aggregated at the VPP level and used as scenarios' input for the proposed optimization problem in Section 4.1.

Eventually, our dataset contains the following fields:

- Upward: The available upward flexibility (in kW) for the given hour.
- Downward: The available downward flexibility (in kW) for the given hour.
- Energy: The total energy (in kWh) associated with the flexibility for that hour.

Figure 3 shows the mean upward and downward flexibility for each hour, along with their 95% confidence intervals, to provide insights into the temporal patterns and variability of flexibility resources throughout the day. This visualizations help identify trends, such as peak flexibility periods and the reliability of flexibility offers, which are crucial for designing robust bidding strategies in energy markets.

5.2. Dataset Preprocessing

The raw data, originally provided in hourly CSV files, underwent several preprocessing steps to prepare it for analysis. First of all, the dataset includes hourly data from the 1st of January 2023 to the 23rd of November 2023, covering a total period of 327 days. Following this, an outlier imputation strategy was implemented to address data anomalies, particularly at month boundaries. Outliers were identified using the Z-score method as suggested in [45]; any data point where a signal's Z-score exceeded a threshold of 1.4 was flagged. However, only outliers occurring within a "valley window" - a specified range of days at the end of one month (from day 26) and the beginning of the next (to day 4) - were targeted for replacement. This selective imputation was designed to correct for boundary effects without altering the bulk of the data.

The replacement values were chosen via a contextual sampling method, similar to the one proposed in [46]. For each outlier, a substitute data point was randomly sampled from a non-outlier period that shared the same weekday/weekend classification and belonged to the same, previous, or next month. This approach was chosen to preserve both the natural variability and the inherent weekly and seasonal patterns of the time-series data, thereby avoiding the over-smoothing that can result from simpler imputation techniques like mean or median replacement. In cases where no suitable replacement candidate was found, the value from the preceding day was used as a fallback.

Figure 4 shows a comparison between the data before and after undergoing the processing steps. To ensure that this selective outlier replacement method did not bias any seasonal pattern, we provide a robustness check of the performed outlier replacement in terms of correlation-based robustness metrics at multiple timescales on each field. We show in Table 1 the results obtained comparing the original dataset, removing the outliers, and the processed dataset. We focus on seasonal bias with monthly, weekly and daily correlation, adding Power Spectral Density (PSD) to verify temporal structure preservation. These results justify the choice of the outlier replacement, since it preserved the intrinsic temporal and seasonal structure. In fact seasonal biases are almost completely preserved, while the PSD values above 94% confirm a good temporal structure preservation [47].

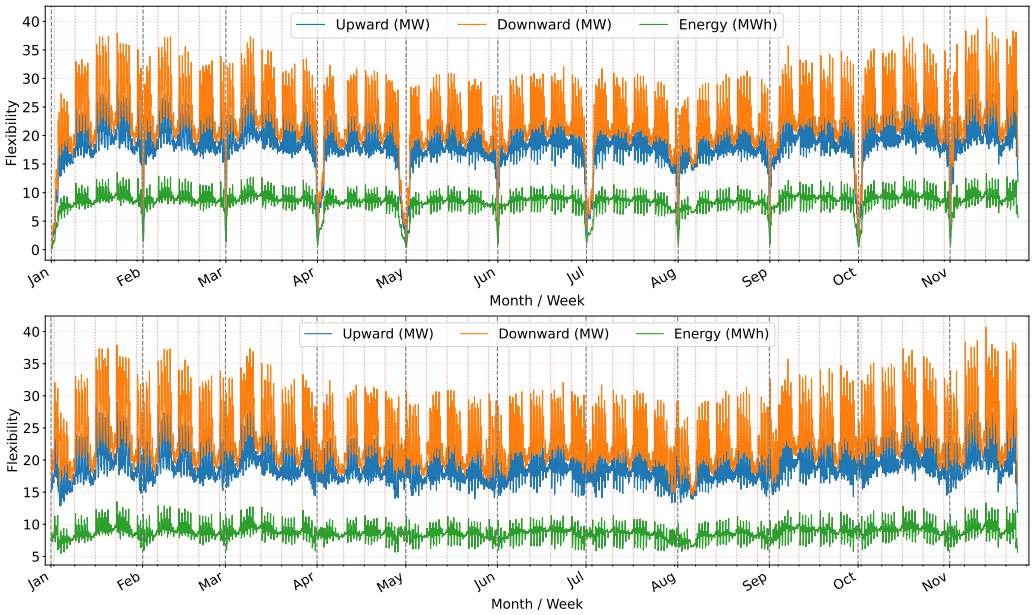

Figure 4: Visualization of the dataset before (top) and after (bottom) the processing steps.

Table 1: Robustness checks of the proposed outlier replacement.

Field	Monthly	Weekly	Daily	PSD
Upward	99.82%	99.97%	99.97%	94.25%
Downward	99.56%	99.99%	99.97%	95.36%
Energy	99.84%	99.81%	99.98%	94.14%

5.3. Penalty scale factor definition

The penalty regimes are completely generalizable as discussed in Section 3.3. The choice of the scale factor depends on the relative importance assigned to penalties in the specific market context. As previously mentioned, we will propose in Appendix B a comparison among different scale factors. In the remainder of the paper, we will instead focus on a fixed scale factor: for the proposed benchmarks, different factors only impact the net revenue, while our model continuously adapt to the corresponding scale factor, as it will be seen in Appendix B. Given the results shown in Appendix B, we consider the choice of the fixed scale factor analysis as reasonable. In particular, the choice of the scale factor is based on domain knowledge and similar

market-specific penalty intensity. According to these considerations, we fix the scale factor at $SF = 2$ (see corresponding penalty regimes' in Figure 1).

5.4. Comparison of Model Performance

We present in this Section the comparison of model performance with respect to several metrics. As previously mentioned, we compare three bidding strategies: an *Analytical* baseline that uses statistical risk thresholds, a *Sample-based* chance-constrained optimization, and a *Penalty-Optimized* approach (PenaltyOpt) that explicitly incorporates penalty costs into its bids. For consistency, we present three PenaltyOpt variants, each optimised for a specific penalty shape (linear, quadratic, and exponential), and evaluate every variant under the same penalty model used in its optimization.

5.4.1. Baseline Comparison: Analytical vs. Sample-Based

Results are consistent with the findings by Herstad *et al.* [26], which reported that an analytical bidding strategy generally outperforms sample-based methods in terms of reliability. In the present analysis, the sample-based model indeed achieves a higher gross revenue by committing more capacity, indicating a greater risk appetite. However, it also incurs substantially higher penalty costs due to more frequent and severe shortfalls. By contrast, the analytical approach is more conservative in its bidding, which limits the occurrence of shortfalls and associated penalties. As a result, after accounting for penalty costs, the analytical strategy realizes a higher net revenue overall (as discussed in Appendix B, this outperformance holds true even for relatively small penalty scale factors, where the analytical model surpasses the sample-based approach not only in net profit but also across other key metrics). This outcome is reflected in Table 2, which shows that the sample-based strategy's gains in gross revenue is offset by greater penalty costs, while the analytical approach achieves a slightly lower gross revenue but smaller penalties, resulting in a higher net revenue.

As shown in Table 3, the sample-based method fails to meet the delivery reliability requirement more frequently, with an out-of-sample violation rate of 14.54%, whereas the analytical approach achieves a significantly lower violation rate of 9.83%. This is again in line with the $\approx$ 10% violation rate observed in the findings by Herstad *et al.* [26]. Table 3 will also be considered when comparing the Penalty-based strategies with the benchmark ones discussed here.

Table 2: Revenue & Penalty Summary (Analytical vs Sample).

Method & Type	**Gross Rev (€)**	**Penalty (€)**	**Net Rev (€)**
Analytical Linear	5,347,018.14	571,318.08	4,775,700.05
Sample-based Linear	5,524,566.54	825,137.12	4,699,429.43
Analytical Quadratic	5,347,018.14	864,272.08	4,482,746.05
Sample-based Quadratic	5,524,566.54	1,432,044.86	4,092,521.69
Analytical Exponential	5,347,018.14	504,300.02	4,842,718.12
Sample-based Exponential	5,524,566.54	822,760.22	4,701,806.32

Table 3: Out-of-sample Violation Rates by Strategy.

Strategy	**Violation Rate (%)**
Analytical	9.83
Sample-based	14.54
Penalty-based (Quadratic)	5.06
Penalty-based (Linear)	8.97
Penalty-based (Exponential)	8.17

The analytical strategy also proves more effective at containing the severity of shortfalls when violations do occur. Figure 5 illustrates the distribution of shortfall magnitudes under each strategy. Notably, the sample-based approach occasionally incurs large shortfalls (on the order of 30%), approaching the penalty termination threshold. In contrast, the shortfalls under the analytical approach are not only less frequent but also significantly milder. For instance, focusing on the extreme shortfalls at 28-30% of the sample-based model, those are contained by the analytical method as we can see from the distribution, stopping at a 22-24% interval. Moreover, comparing the two graphs in Figure 5, it can be seen that Sample has generally higher occurrence in absolute value with respect to Analytical (as expected from the higher violation rate), meaning that the severe shortfalls (more than 20% violation rate) are also more numerous in terms of absolute quantities. This behaviour is shown in all the shortfall distribution, where the errors in the analytical method are typically confined closer to the 10% tolerance limit. This shift in the shortfall profile reflects the analytical model's more risk-averse stance, mitigating the impact of each violation. Consequently,

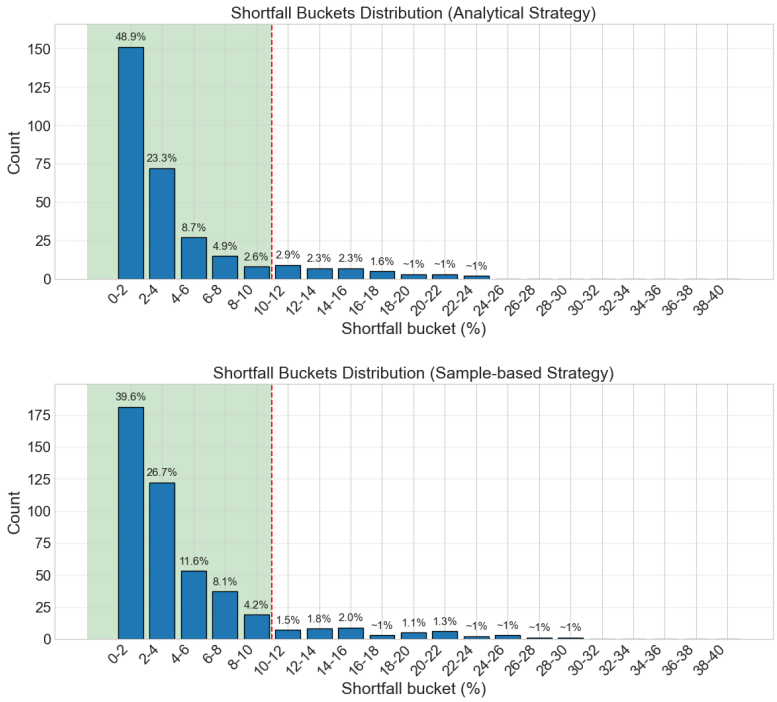

Figure 5: Percentage of violations of the Analytical (top) and Sample-Based (bottom) models grouped in buckets according to their shortfall.

the total penalties incurred by the analytical strategy are far lower. For instance, under a quadratic penalty scheme (where the penalty cost escalates with the square of the shortfall), the analytical model's penalty cost is about 40% lower than that of the sample-based approach. These findings highlight how the analytical strategy's cautious allocation leads to improved reliability and a higher net benefit compared to the sample-based strategy.

5.4.2. Bidding profiles

Figure 6 compares the hourly bidding patterns of each strategy against the estimated available flexibility profile considering a quadratic penalty regime. All three methods successfully track the general shape of the flexibility supply curve, concentrating their offers to align with the daily peaks of available capacity (mid-morning and early afternoon). The Analytical and PenaltyOpt strategies appear to capture the finer-grained peaks and valleys slightly better, adapting more closely to the system's hourly capabilities.

As expected from its design, the Sample-based strategy (dash-dot 'x' line)

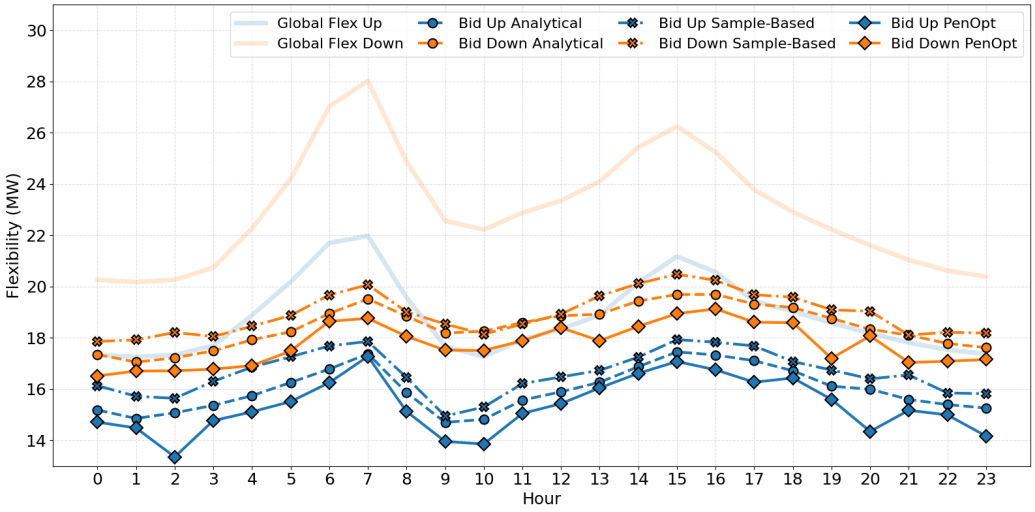

Figure 6: Bidding Profiles of the different models compared to the estimated availability profile. As an example, quadratic penalization is taken into account.

is consistently the most aggressive, offering the highest capacity in almost every hour. This results in higher gross revenues as discussed but also reveals a more rigid bidding pattern that is less adaptive to the hourly shape of the flexibility curve. This is a likely consequence of its scenario-driven MILP formulation, which optimizes against the entire set of historical samples rather than a statistical distribution.

In contrast, the PenaltyOpt strategy (solid diamond line, shown with a quadratic penalty objective) demonstrates a more adaptive, risk-averse stance. While it is generally more conservative than the Analytical model, its conservatism is not uniform. The model appears to have learned which hours are riskiest, as it bids significantly lower at specific times (e.g., hours 9, 10, 17, 20, and 23) to avoid incurring large shortfall penalties.

A notable observation across all models is the difference in the bidding gap between the upward and downward services. While the upward bids (blue lines) are relatively close to the "Global Flex Up" profile, all three downward bids (orange lines) are significantly lower than the "Global Flex Down" profile. This suggests a much higher perceived risk or variance in the downward flexibility. Given this dataset is from a commercial fleet, this is plausible: downward flexibility (i.e. charging) is highly dependent on stochastic factors like vehicle return times and their state-of-charge upon arrival. This can also

be seen in Figure 3, where the downward flexibility 95% confidence interval range results bigger than the upward's. Faced with this higher variance, all models (including the risk-aware Analytical and PenaltyOpt) adopt a more cautious and conservative bidding stance for the downward service.

5.4.3. Reliability

Table 3 shows the out-of-sample violation rates for each strategy. While all five maintain a high level of reliability on the test set, there are visible differences in the methods. The PenaltyOpt method, considering a quadratic penalty in the objective function, achieves a violation rate of just 5.06% consistent with its design for stringent delivery guarantees. The linear and exponential PenaltyOpt calibrations follow closely the Analytical results, posting violation rates of 8.97% and 8.17%, respectively. The behavior of these two penalty calibrations is similar because no dramatically large shortfalls were registered in the test set; consequently, the steepest part of the exponential curve was never triggered. However, the slight difference between them is due to the few shortfall observations exceeding 20%, a range where, as shown in Figure 1, the exponential penalty begins to exceed the linear one.

The difference between the Analytical and PenaltyOpt models becomes even more evident when examining the distribution of shortfall magnitudes (Figure 5 vs. Figure 7). These figures group shortfall occurrences into severity buckets, revealing how the PenaltyOpt strategy's risk profile adapts to the specific penalty shape it optimizes against.

The quadratic penalty objective (Figure 7, middle) induces the most dramatic adaptation. In this scenario, the model learns that large shortfalls are prohibitively expensive and adopts a highly risk-averse strategy by completely cutting off the tail of the distribution. It experiences no shortfalls greater than 20%. Furthermore, because the overall violation rate for this model is the lowest (as shown in Table 3), the counts in all violation buckets are relatively smaller.

The other two PenaltyOpt models show more nuanced behaviours. The PenaltyOpt-Linear model (Figure 7, top) is actually more aggressive than the Analytical baseline (Figure 5, top). It learns that the penalty for underdelivery is only proportional and is therefore less risk-averse, allowing shortfalls to extend into the 30-32% bucket, a range the Analytical model avoids. This demonstrates a clear trade-off, accepting occasional larger shortfalls in exchange for higher average bids. Conversely, the PenaltyOpt-Exponential model (Figure 7, bottom) is slightly more conservative than the Analytical

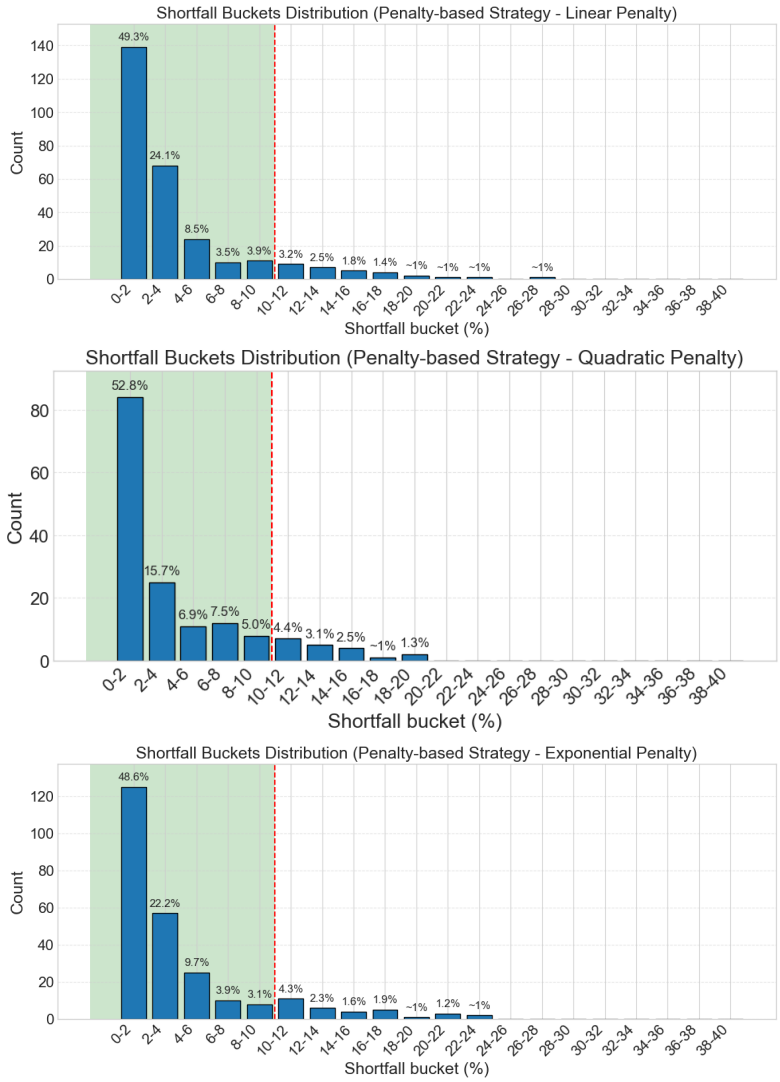

Figure 7: Percentage of violations of the Penalty-Based models (one for each penalty regime) grouped in buckets according to their shortfall.

baseline. It learns to be cautious, curtailing its maximum shortfall at the 24-26% bucket. This behavior highlights the model's sensitivity to the severe costs associated with large shortfalls in this regime, even when such events are rare.

Table 4: Revenue & Penalty Summary with penalty type braces and vertical labels.

	Method & Type	Gross Rev (€)	Penalty (€)	Net Rev (€)
Lin.	Analytical	5,347,018.14	571,318.08	4,775,700.05
	Sample-based	5,524,566.54	825,137.12	4,699,429.43
	Penalty-based	5,281,695.39	462,313.23	4,819,382.15
Quad.	Analytical	5,347,018.14	864,272.08	4,482,746.05
	Sample-based	5,524,566.54	1,432,044.86	4,092,521.69
	Penalty-based	5,136,677.76	353,746.79	4,782,930.98
Exp.	Analytical	5,347,018.14	504,300.82	4,842,718.12
	Sample-based	5,524,566.54	822,768.22	4,701,886.32
	Penalty-based	5,286,996.46	429,223.18	4,857,773.28

5.4.4. Revenues and penalties

The financial outcomes of each strategy under different penalty regimes are summarized in Table 4. We see a clear trade-off between aggressive bidding and penalty costs. Overall we can observe that the PenaltyOpt model outperforms the base line ones under each regime. In particular, under a *linear penalty* (where the cost grows in direct proportion to shortfall), the Sample-based strategy achieves the highest gross revenue (approximately €5.24M on the test set) by bidding the most aggressively, compared to about €5.34M for Analytical and €5.28M for PenaltyOpt. However, Sample-based also incurs the largest total penalty (€825k) in the linear regime, roughly 1.5 times the Analytical strategy's penalty (€571k) and around two times PenaltyOpt's (€462k). These hefty penalty deductions erase Sample's revenue advantage: its net revenue comes out slightly low compared to the others (€4.70M), despite higher gross earnings. PenaltyOpt's net (€4.82M) is slightly better than the Analytical-based (€4.78M). This indicates that the extra income from more aggressive bidding can be almost entirely offset by proportional penalty costs.

In the *quadratic penalty* scenario (which punishes larger deviations more severely), the differences sharpen. The Sample-based approach, which does not explicitly limit tail-risk, ends up paying about €1.43M in penalties, nearly 26% of its €5.24M gross revenue, causing its net profit to crash to €4.09M. Analytical's more cautious bidding incurs a moderate €864k penalty, yielding a net of €4.48M. Meanwhile, PenaltyOpt (optimized for a

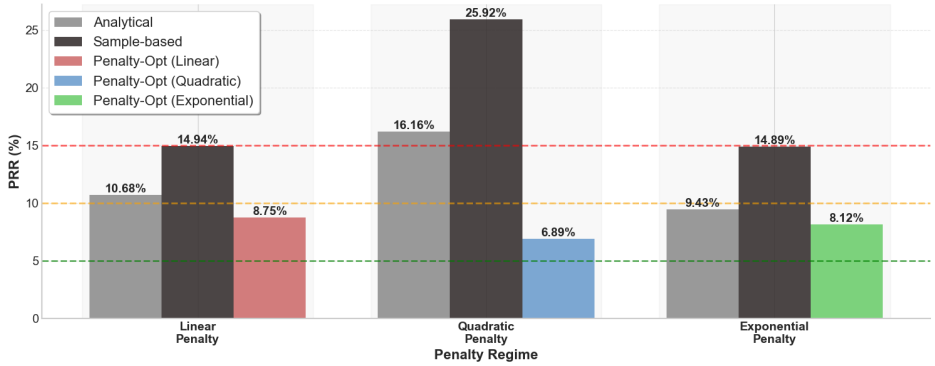

Figure 8: PRR for each penalty regime. This metric measures economic efficiency, i.e. how much of your revenue is lost to penalties.

quadratic penalty) dramatically curtails penalty costs to €354k and achieves the highest net revenue of €4.78M. By accounting for the steeply increasing cost of larger shortfalls, PenaltyOpt preserves more of its earnings than either baseline.

Under the *exponential penalty* regime, which imposes extremely severe costs for big shortfalls, none of the strategies experienced catastrophic penalties. In our tests, no hourly shortfall exceeded 40% of the promised energy, so none of the bids triggered the exponential penalty's extreme tail (which would correspond to contract termination or exorbitant fees). Accordingly, the incurred penalties remained moderate: roughly €823k for Sample-based, €504k for Analytical, and €429k for PenaltyOpt. Net revenues under exponential penalties ended up close to those under linear penalties: PenaltyOpt was highest at €4.86M, Analytical next at €4.84M, and Sample-based lowest at €4.7M.

5.5. Model Comparison under Advanced Metrics

As introduced in Section 3.3.1, several additional metrics allow a wider perspective on both reliability and economic performance. In Figure 8 we show the PRR for each model (bar color) for each penalty regime (x-axis tick). We also add on the graph three thresholds at 15%, 10% and 5%, indicating aggressive bidding, balanced bidding and conservative bidding respectively. We see that the Sample-based strategy is too aggressive regardless from the penalty regime, meaning that the method will incur severe penalty risk, as seen in the previous results. In fact, Sample-based bidding doesn't

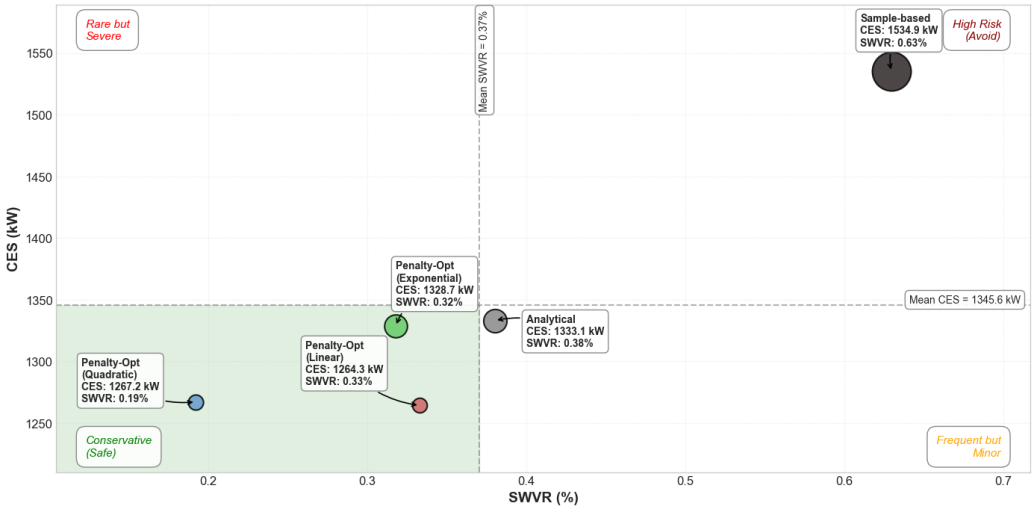

Figure 9: Combined visualization of CES and SWVR. These two metrics together provide an integrated risk assessment of each model.

consider the penalty regime, thus the PRR is rather a measure of the entity of the penalties on the revenue in each penalty regime, considering the shortfall distribution in Figure 5 (bottom). The same holds for the Analytical strategy, that results less aggressive in the linear and the exponential regime, but still too aggressive in the quadratic regime (see Figure 5 above for the corresponding shortfall distribution). Instead, the PenaltyOpt method, integrating the corresponding penalty growth rate, manages to keep a balanced bidding for each case (8.75% for linear, 6.89% for quadratic and 8.12% for exponential). Again, the PenaltyOpt demonstrates its ability, considering the penalty shape, to perform an efficient trade-off between revenues and penalties. In PenaltyOpt, the shortfall distributions depend on the regime (as seen in Figure 7), in fact the PRR in a quadratic penalty is particularly lower than the Analytical, due to the severity of the violations from low shortfall values in that case (see Figure 1).

In Figure 9, we propose an integrated analysis on the risk that each model face. In order to do this analysis, two metrics are combined. On one hand, CES represents the average violation size in terms of power, while SWVR represents the violation rate weighted by its severity (similar to the risk definition, probability times consequences' magnitude). We identify in this combined analysis four main regions according to the average CES and

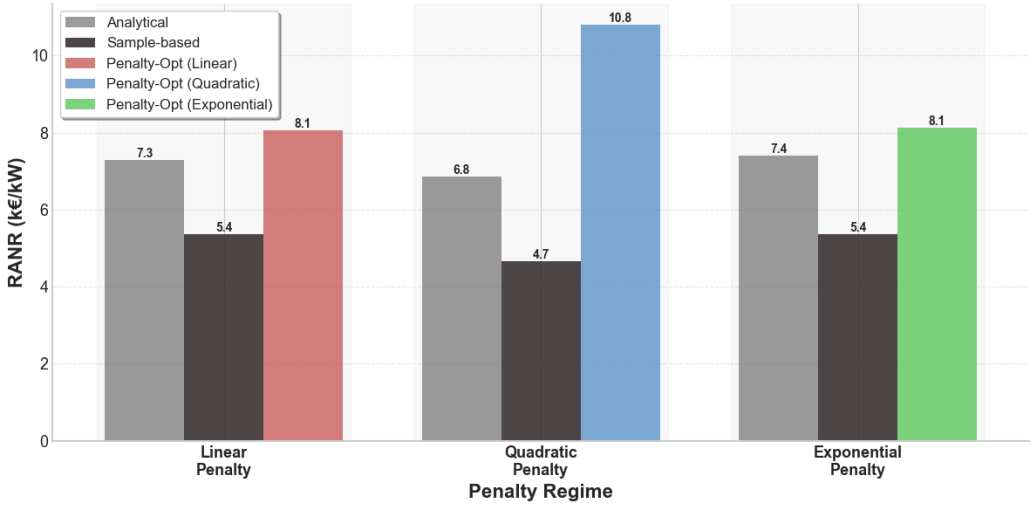

Figure 10: RANR for each penalty regime. It represents the net revenue earned per unit of risk.

SWVR. All three PenaltyOpt models belong to the conservative region (CES and SWVR lower than their average), with CES ranging from 1264.3 kW (linear) to 1328.7 kW (exponential) and SWVR from 0.19% (quadratic) to 0.33% (linear). Instead, the Analytical model has a frequent but not-so-severe shortfall occurrence, with a 1338.1 kW CES and a 0.38% SWVR. Finally, the Sample-based approach yields the worst result in terms of risk assessment, with a 1534.9 kW CES and a 0.63% SWVR (frequent and severe shortfalls). As a final remark, Sample-based should just be considered when penalties are very low with respect to revenues (low scale factor), Analytical is a better choice but still not enough risk-averse, while PenaltyOpt models achieve good risk management regardless from the penalty regime.

Finally, we show in Figure 10 the RANR for each model operating in every penalty regime. This analysis aims to evaluate the efficiency of risk-taking, condensing the information regarding economic performance, shortfall magnitude and risk adversity. PenaltyOpt yields the best risk adjusted return, where the risk is measured as the standard deviation of the shortfalls, in each penalty regime, while Sample-based results to be the worst. Analytical performs fairly good for linear and exponential regimes (-10.6% and -9.9% with respect to the corresponding PenaltyOpt, respectively), while it obtains bad results for the quadratic regime (-57.8% versus the PenaltyOpt with

quadratic penalty). It is also interesting to notice that linear and exponential regimes results in almost equal values of RANR, while the quadratic penalty RANRs are different. In fact, the quadratic penalty turned out to be the most critical regime, highlighting our model ability to carry out an effective hedging against the shortfall risks. This can be seen by the PenaltyOpt having the highest RANR for quadratic penalty, while Analytical and Sample-based yield lower results compared to other penalties. This can be justified by the PenaltyOpt ability to adjust to high initial penalties, while the other two benchmark models undergo this condition passively.

5.5.1. Mechanism-level explanation of PenaltyOpt performance

Unlike the Analytical and Sample-based strategies, our proposed model explicitly integrates penalties growth rate in the optimizer's search dynamics. That is, the algorithm internalizes the marginal penalty gradient at each step, thus learning to hedge against the rising risk of large shortfalls by dynamically trading off penalty exposure against potential revenue gains (see Figure 9 and Figure 10). As the penalty functions grow rapidly with deviation magnitude, the optimization search space becomes steeper in high-risk regions, driving the solution toward safer bidding strategies that minimize tail-risk exposure. This can be especially be seen in penalties with high initial values, i.e. quadratic, where the PenaltyOpt method is able to keep low the shortfall magnitude and occurrence (see Figure 7 and Figure 8). This mechanism explains both the reduced violation rates (Table 3) and the much lower penalty costs (Table 4). By replacing hard risk constraints with continuous penalties, PenaltyOpt achieves smoother control in high-risk periods, mitigating large shortfalls while preserving flexibility in lower-risk hours. In contrast, the Analytical model relies on static risk margins that cannot adapt to the time-varying distribution of uncertainty, and the Sample-based approach treats risk implicitly through stochastic sampling, which may overestimate profitable but high-penalty configurations.

6. Conclusions and future work

This paper presented a novel penalty regime integration within a penalty-aware bidding strategy for EV aggregators in ancillary service markets. The study began by framing the strategic role of Virtual Power Plants in the European energy landscape, emphasizing recent market trends and business directions. It then focused the Italian regulatory context, focusing on the

TIDE framework and its implications for aggregator participation. Building on this foundation, we formulate the problem as a penalty-integrated optimization model that explicitly incorporated under-delivery penalty costs into the bidding process, providing a new analytical approach to balance reliability and revenue. The proposed novelty is the characterization and consideration of penalties' growth rates inside the framework. Simulation results demonstrated that this penalty-aware method outperformed two baseline strategies (Analytical and Sample-based) that did not explicitly account for penalty costs, in terms of net revenue and reliability. By accounting for penalty risks, the proposed model achieved nearly the same high delivery success rate as the risk-averse analytical model, while improving net profit, especially under stricter (non-linear) penalty regimes. Indeed, the proposed model allows these performances with a lower capital risk that translates in a better risk-taking approach.

However, several limitations and potential enhancements remain. First, integrating the charging and bidding decisions with broader energy market participation (e.g. day-ahead market bidding) and real-time balancing price signals would result in a more comprehensive optimization framework, thereby improving the model's real-world applicability. We plan to extend this framework in future work to capture more complex market mechanisms and to incorporate additional benchmark models (e.g., reinforcement learning). Second, the approach has yet to explicitly account for temporal patterns and seasonality. Using multiple years of data would allow the model to learn seasonal variations in energy demand (since EV charging behavior and electricity consumption can vary significantly with seasonal weather changes). Possible future work on this matter include training season-specific models or employing a rolling-window training scheme. By addressing these temporal dynamics and sequential decision-making aspects, future work can further improve the forecasting accuracy and robustness of the model, enhancing its practical effectiveness. Finally, since this work focused on what can be seen as an upper-layer to a scheduling strategy, future work will address the said scheduling layer to improve practical applicability. This advancement will have to consider detailed EV and grid impact modeling, that was beyond the scope of this work, but would be crucial to address the VPP dispatching phase.

Acknowledgment

This work has been conducted in the framework of the XX cycle of Alta Scuola Politecnica (ASP), in collaboration with Politecnico di Milano, Politecnico di Torino and Free2move eSolutions S.p.A.

Appendix A: Distributional Diagnostics for the Tail Fitting

The Analytical (EVT-Based) bidding strategy, described in Section 3.1, critically depends on accurately modelling the extreme lower tail of the available flexibility distributions. This appendix provides the diagnostic validation for our choice of the Weibull distribution. Our analysis focused on the 10% lower tail of the flexibility distributions (Upward, Downward, and Energy) for each of the 24 hours. To apply standard tail-fitting techniques, we transformed the data by considering the exceedances below the 10th percentile.

We then fitted three common EVT distributions to this tail data: the Weibull distribution, the Generalized Pareto Distribution (GPD) and the Generalized Extreme Value (GEV) distribution. The quality of the fit for each model was evaluated over the 24-hour period using two standard metrics: the Akaike Information Criterion (AIC) for model comparison and the Kolmogorov-Smirnov (KS) test for goodness-of-fit.

The diagnostic results confirmed the suitability of the Weibull distribution. Indeed, as summarized in Table 5, the Weibull distribution demonstrates an exceptionally strong fit to the empirical tail data. For all three flexibility types, the model passed the KS test 100% of the time (p-value > 0.05) across all 24 hours. The high median p-values (e.g., 0.8364 for Upward, 0.7486 for Downward) indicate a very strong statistical agreement.

The AIC comparison, illustrated in Figure 11 for the Upward flexibility case, provides further insight. The AIC values for the Weibull (blue bars) and GPD (orange bars) models are consistently low and very similar to each other. In contrast, the GEV model (green bars) is systematically worse, exhibiting a significantly higher AIC in almost every hour, suggesting it is an unnecessarily complex or poor-fitting model for this data.

Based on its 100% pass rate on the KS test and its consistently low AIC score (comparable to the GPD), the Weibull distribution was selected as a robust and parsimonious choice for the Analytical (EVT-Based model).

Table 5: Weibull Goodness-of-Fit Summary (24-hour Analysis).

Flexibility Type	Median KS p-value	Test Pass Rate ($p > 0.05$)
UPWARD	0.8364	100.0%
DOWNWARD	0.7486	100.0%
ENERGY	0.8234	100.0%

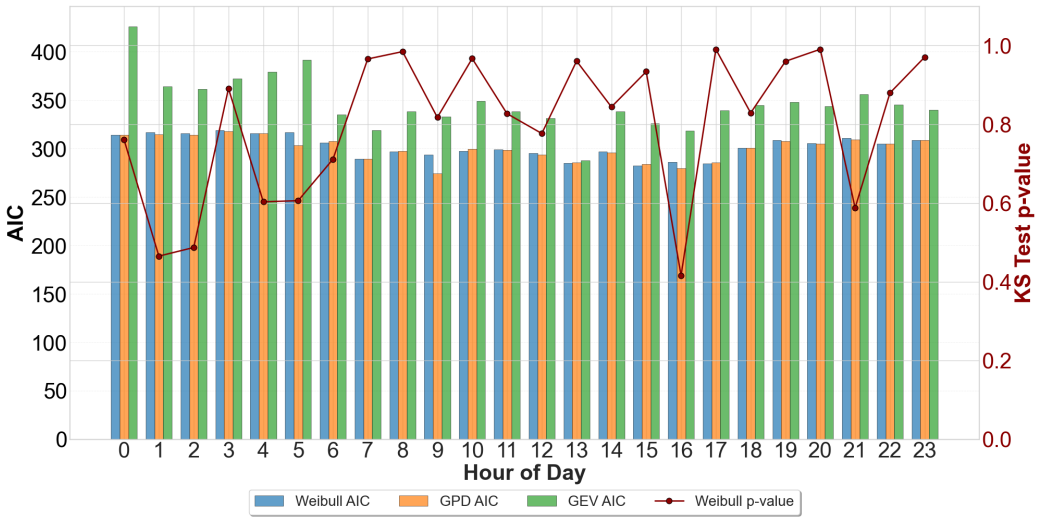

Figure 11: Distributional diagnostics for the Upward flexibility tail over 24 hours. The plot compares AIC scores (bars) for the Weibull, GPD, and GEV models, alongside the corresponding KS-test p-value (red line) for the Weibull fit, confirming its statistical validity.

Appendix B: Scale Factor Generalization

The main analysis in Section 5 uses a fixed penalty scale factor (SF) of 2.0. This appendix provides a more detailed analysis of the penalty structures, as promised in Section 5.3, by examining their behaviour across a wider range of scale factors (SF $= 1.0, 2.0, 3.0, 4.0$ and 5.0).

The scale factor is a linear multiplier that scales the financial "harshness" of all three penalty regimes, which were first introduced in Figure 1. However, due to the non-linear nature of the quadratic and exponential functions, increasing the SF does not just scale all penalties uniformly. It also amplifies the delta (monetary difference) between the non-linear penalties and the linear benchmark for any fixed shortfall percentage. This effect is explicitly visualized in Figure 12. These heatmaps illustrate the mone-

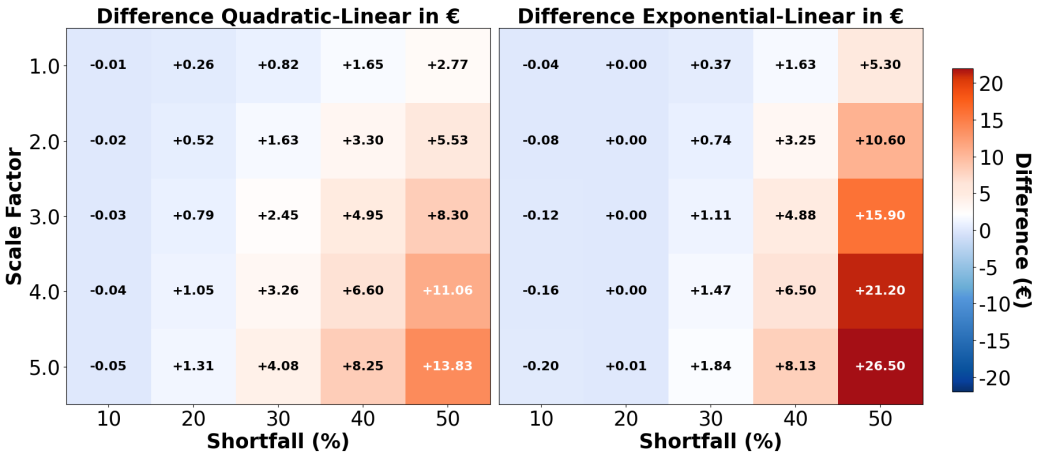

Figure 12: Monetary difference (€) between penalty regimes, using Linear as the baseline, across various Scale Factors (y-axis) and Shortfall percentages (x-axis).

tary difference between the penalty regimes, using the linear penalty as the reference baseline. The selected SF values cover a wide range of potential market scenarios. By analysing the heatmaps, we can observe the distinct characteristics of each penalty shape by reading across the rows (fixed SF, increasing shortfall) and down the columns (fixed shortfall, increasing SF).

Analysing the columns confirms the scaling effect: for any fixed shortfall percentage, the absolute monetary difference between the non-linear and linear penalties increases monotonically as the Scale Factor increases. This highlights how a harsher market (a higher SF) amplifies the financial consequences of non-linear penalty structures. Analysing the rows reveals the different growth rates, following the rules imposed in the calibration presented in Section 3.3.

This analysis validates the core thesis of the paper: the performance of the baseline models (Analytical and Sample-based) is highly sensitive to the penalty regime, while the PenaltyOpt model robustly adapts to changing market severity. A clear trend emerges from the economic results shown in Figure 13, where linear (top), quadratic (middle) and exponential (bottom) regimes are evaluated with increasing SF. This threefold figure allow us to i) analyse the different regime impact on similar SF (vertically) and ii) evaluate the increasing SF effect in each regime (horizontally). We will employ the former perspective. SF $= 1$ scenario represents a market with very low penalties, where the cost of a shortfall is not high enough to jus-

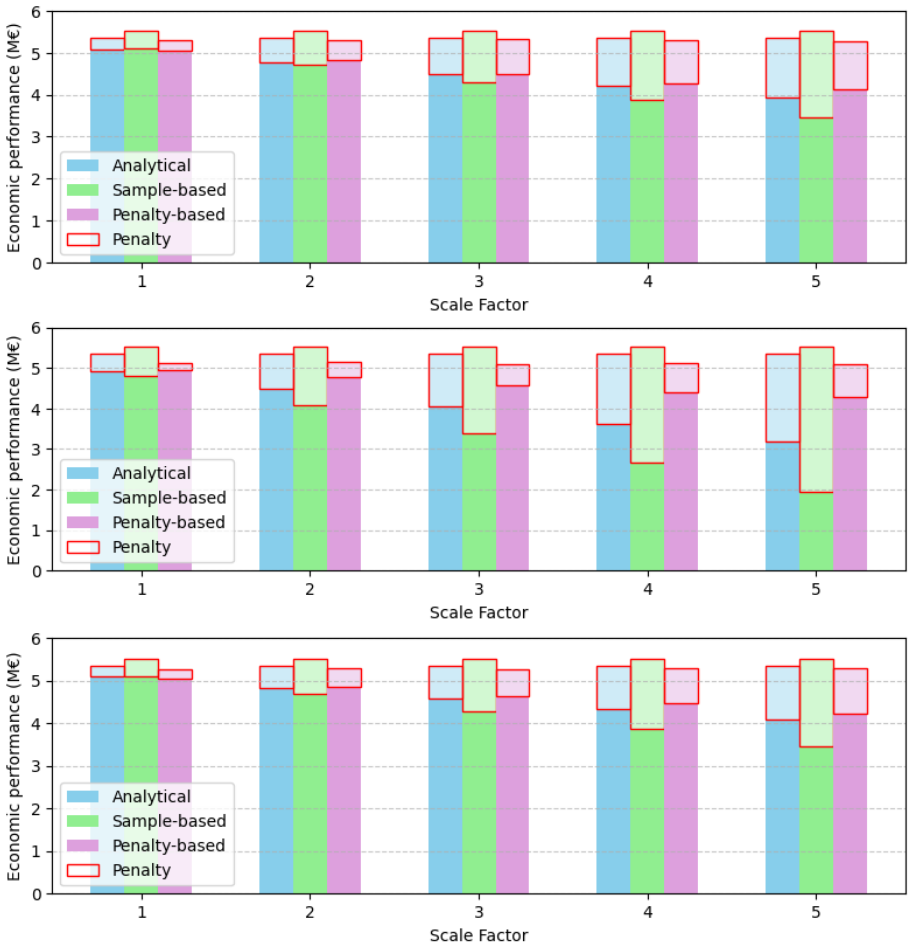

Figure 13: Economic performance of each model with respect to increasing scale factor in Linear (top), Quadratic (middle) and Exponential (bottom) penalty regime. We show as lighter bars the gross revenue, as darker bars the net revenue (that is the gross minus the penalty, shown as the red portion of the gross revenue).

tify a conservative bidding strategy. In this specific, lenient environment, the aggressive Sample-based strategy achieves the highest net revenue in the Linear (top) and Exponential (bottom) regimes, as its high gross revenue outpaces its modest penalties. However, even in this low-penalty scenario, the PenaltyOpt models already demonstrate their efficiency by incurring the lowest absolute penalty costs.

As the scale factor grows, making penalties progressively more important, the financial superiority of the PenaltyOpt strategy becomes domi-

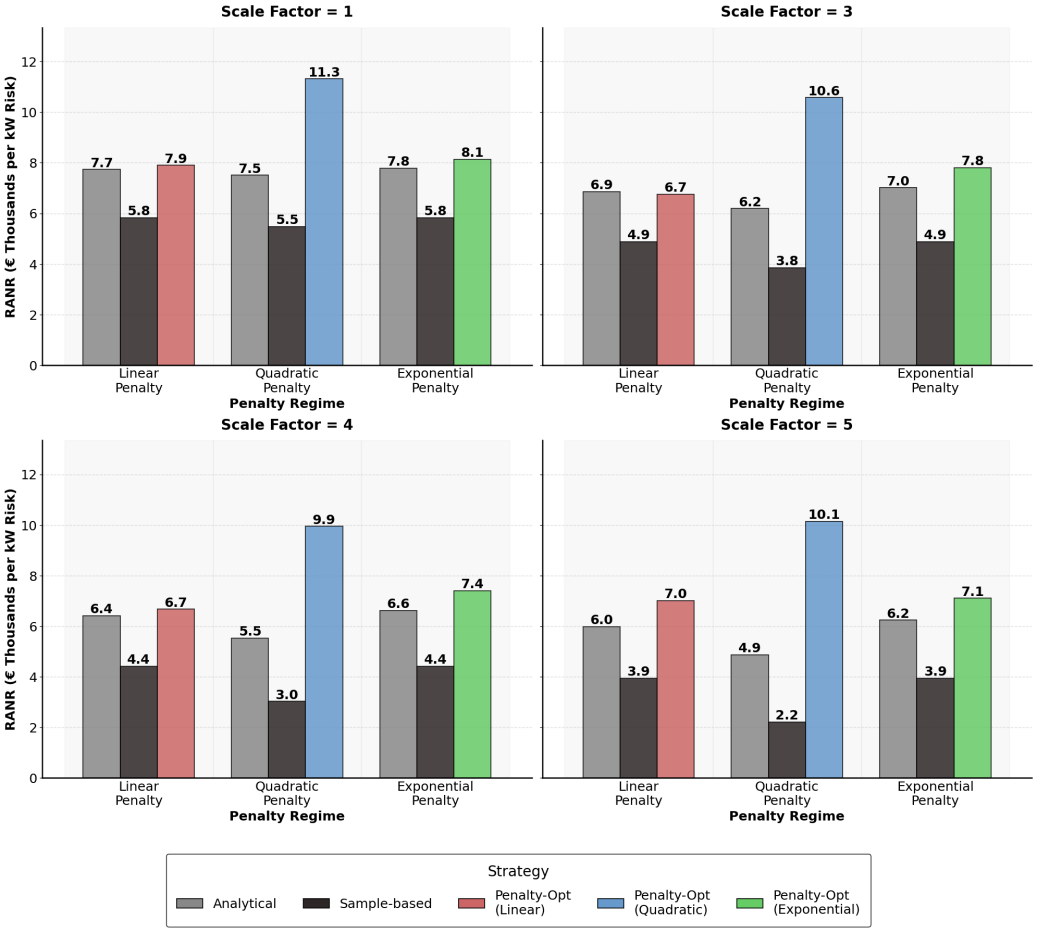

Figure 14: RANR for each penalty regime and scale factor

nant. In the moderate SF = 3 regime, PenaltyOpt outperforms the Analytical model in all three penalty types. By SF = 4 and SF = 5, the gap widens significantly. For instance, under the severe Quadratic regime at SF = 5, the PenaltyOpt model achieves a net revenue of €4.27M, whereas the Analytical model's profit collapses to €3.18M and the Sample-based model's to just €1.94M. This demonstrates the critical importance of integrating penalty awareness as market conditions become harsher.

The risk-adjusted metrics confirm the PenaltyOpt model's superior efficiency, even in scenarios where its net revenue is not the highest. Figure 14 shows that the PenaltyOpt models (red, blue, and green bars) consistently

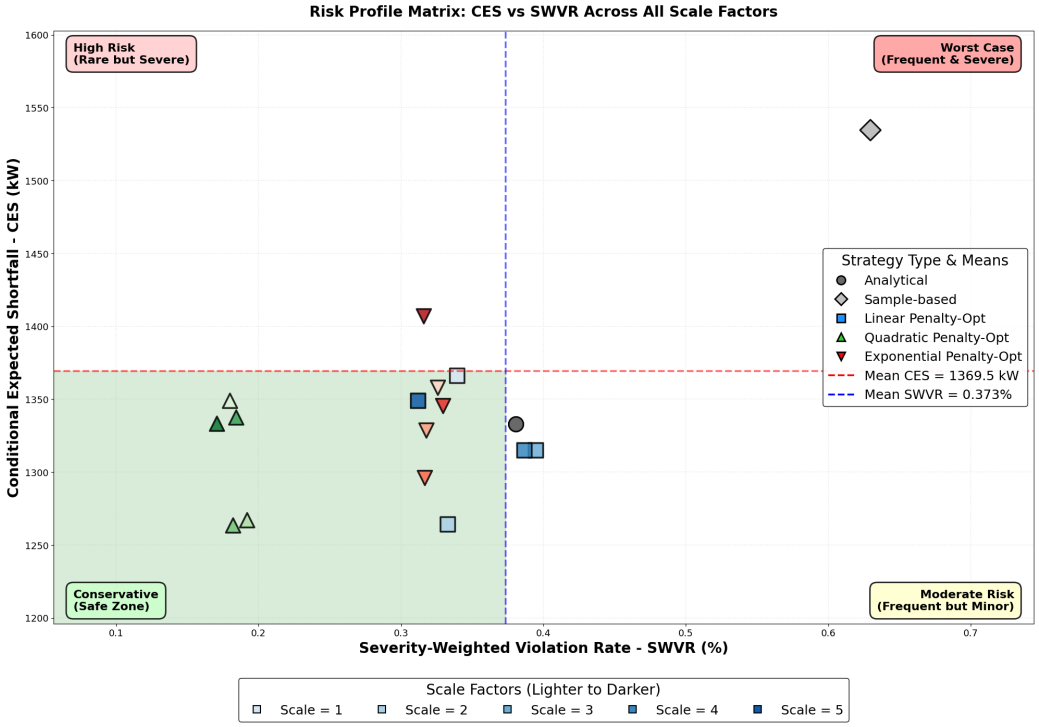

Figure 15: Combined visualization of CES and SWVR for different values of scale-factors

deliver the highest risk-adjusted returns (RANR) across all scale factors and all penalty regimes. Even at SF = 1, where the Sample-based model had a slight net revenue advantage, PenaltyOpt's RANR is significantly higher, confirming it as a more capital-efficient and stable strategy. The blue bar (Penalty-Opt Quadratic) achieves the highest RANR in all cases, illustrating its exceptional ability to manage risk. Figure 15 provides a comprehensive risk assessment, plotting all model variations across all scale factors. The Sample-based strategy (grey diamond) is isolated in the "Worst Case" quadrant, characterized by both frequent and severe shortfalls. The Analytical model (squares) clusters in the "Moderate Risk" zone. In stark contrast, all PenaltyOpt models (triangles, inverted triangles, and squares) are mostly tightly grouped within the "Conservative (Safe Zone)," demonstrating consistently low shortfall severity and frequency, regardless of the scale factor. The Penalty-Opt Quadratic (green triangles) achieves the best risk performance overall, pushing furthest into the safe corner with the lowest SWVR, confirming its power to adapt to and hedge against even the harshest penalty

regimes.

Finally, the choice of SF = 2 for the main paper's analysis is validated by these findings. SF = 1 represents an unlikely lenient market where penalties are almost negligible. Conversely, SF = 4 and SF = 5 represent very severe markets. SF = 2 serves as a balanced, realistic regime where penalties are meaningful but not catastrophic. These results show that even in this moderate scenario, the advantages of the PenaltyOpt model are already clear, both in absolute net revenue (as shown in Table 4) and in superior risk-management performance (as shown here). This trend of outperformance only becomes more pronounced as the penalty severity (SF) increases.

References

[1] International Energy Agency (IEA). *Digitalization and Energy*. OECD Publishing, Paris, 2017.

[2] F. Teng, D. Pudjianto, and G. Strbac. Assessment of the value of flexibility of power plants in low-carbon electricity systems. In *13th IET International Conference on Developments in Power System Protection (DPSP)*, pages 1–6, 2014.

[3] Mateus Kaiss, Yihao Wan, Daniel Gebbran, Clodomiro Unsihuay Vila, and Tomislav Dragičević. Review on virtual power plants/virtual aggregators: Concepts, applications, prospects and operation strategies. *Renewable and Sustainable Energy Reviews*, 211:115242, 2025.

[4] Abdelrahman Ayad and François Bouffard. Enabling system flexibility in smart grid architecture. *IEEE Transactions on Engineering Management*, 72:1892–1908, 2025.

[5] International Energy Agency (IEA). *Empowering Cities for a Net Zero Future: unlocking resilient, smart, sustainable urban energy systems*. IEA, Paris, 2021.

[6] International Energy Agency (IEA). *Grid Integration of Electric Vehicles: a manual for policy makers*. IEA, Paris, 2022.

[7] M. R. H. Mojumder, F. A. Antara, M. Hasanuzzaman, B. Alamri, and M. Alsharef. Electric vehicle-to-grid (v2g) technologies: Impact on the power grid and battery. *Sustainability*, 14(21):13856, 2022.

[8] Xiyun Yang and Yanfeng Zhang. A comprehensive review on electric vehicles integrated in virtual power plants. *Sustainable Energy Technologies and Assessments*, 48:101678, 2021.

[9] Maher F. Mekky and Alan R. Collins. The impact of state policies on electric vehicle adoption -a panel data analysis. *Renewable and Sustainable Energy Reviews*, 191:114014, 2024.

[10] I. Pavić, H. Pandžić, and T. Capuder. Electric vehicle aggregator as an automatic reserves provider under uncertain balancing energy procurement. *IEEE Transactions on Power Systems*, 38(1):396–410, 2023.

[11] Federico Silvestri, Seyed Mahdi Miraftabzadeh, Michela Longo, and Dario Zaninelli. Contextual analysis of battery electric vehicles' adoption in italy. *Energies*, 18(13), 2025.

[12] Reshmi Chandra, Suman Moitra, Jinia Datta, Bishaljit Paul, and Chandan Kumar Chanda. Resolving uncertainty with decisions for electric vehicle aggregators. In *2024 4th International Conference on Emerging Frontiers in Electrical and Electronic Technologies (ICEFEET)*, pages 1–6, 2024.

[13] Nanda Kishor Panda and Simon H. Tindemans. Efficient quantification and representation of aggregate flexibility in electric vehicles. *Electric Power Systems Research*, 235:110811, 2024.

[14] Mark Jenkins and Ivana Kockar. Electric vehicle aggregation model: A probabilistic approach in representing flexibility. *Electric Power Systems Research*, 213:108484, 2022.

[15] ARERA. Testo integrato del dispacciamento elettrico (tide), deliberazione 345/2023/r/eel (rev.3). Technical report, Autorità di Regolazione per Energia Reti e Ambiente, 2025. Efficace dal 1 gennaio 2025.

[16] ARERA. Orientamenti relativi alla partecipazione dei veicoli elettrici ai servizi di dispacciamento, per il tramite delle infrastrutture di ricarica dotate di tecnologia *vehicle-to-grid*. Technical report, Autorità di Regolazione per Energia Reti e Ambiente, 2020.

[17] Yanchong Zheng, Ziyun Shao, Xiang Lei, Yujun Shi, and Linni Jian. The economic analysis of electric vehicle aggregators participating in

energy and regulation markets considering battery degradation. *Journal of Energy Storage*, 45:103770, 2022.

[18] Jianlin Yang, Fei Fei, Mingwei Xiao, Aili Pang, Zheng Zeng, Li Lv, and Ciwei Gao. A noval bidding strategy of electric vehicles participation in ancillary service market. In *2017 4th International Conference on Systems and Informatics (ICSAI)*, pages 306–311, 2017.

[19] Álvaro García-Cerezo, Luis Baringo, David Bonilla, and Javier García-González. Building bidding curves for an ev aggregator via stochastic adaptive robust optimization. In *2024 International Conference on Smart Energy Systems and Technologies (SEST)*, pages 1–6, 2024.

[20] T. Ghose, H. W. Pandey, and K. R. Gadham. Risk assessment of microgrid aggregators considering demand response and uncertain renewable energy sources. *Journal of Modern Power Systems and Clean Energy*, 7:1619–1631, 2019.

[21] Yanchong Zheng, Hang Yu, Ziyun Shao, and Linni Jian. Day-ahead bidding strategy for electric vehicle aggregator enabling multiple agent modes in uncertain electricity markets. *Applied Energy*, 280:115977, 2020.

[22] Saeed Shojaabadi, Vahid Talavat, and Sadjad Galvani. A game theory-based price bidding strategy for electric vehicle aggregators in the presence of wind power producers. *Renewable Energy*, 193:407–417, 2022.

[23] Jean-Michel Clairand. Participation of electric vehicle aggregators in ancillary services considering users' preferences. *Sustainability*, 12(1), 2020.

[24] Youngkook Song, Yeonouk Chu, Yongtae Yoon, and Younggyu Jin. Virtual power plant bidding strategies in pay-as-bid and pay-as-clear markets: Analysis of imbalance penalties and market operations. *Energies*, 18(6), 2025.

[25] Youngkook Song, Myeongju Chae, Yeonouk Chu, Yongtae Yoon, and Younggyu Jin. Impact of penalty structures on virtual power plants in a day-ahead electricity market. *Energies*, 17(23), 2024.

[26] T. R. Herstad, J. Kazempour, L. Mitridati, and B. Zwart. Bidding in ancillary service markets: An analytical approach using extreme value theory. *arXiv preprint*, 2024.

[27] G. A. Lunde, E. V. Damm, P. A. V. Gade, and J. Kazempour. Aggregator of electric vehicles bidding in nordic fcr-d markets: A chance-constrained program. *IEEE Transactions on Power Systems*, 2024. Also available on arXiv:2412.02308.

[28] Bordin Flavio, Marco Magnanini, Marco Ronchetti, Lucio Antonio Rosi, Riccardo Ramaschi, Julien Rappe, Vinicio Lupo, Sonia Leva, and Tania Cerquitelli. Scalable optimization of electric vehicle fleets in virtual power plants: Centralized versus decentralized implementation. In *2025 IEEE International Conference on Environment and Electrical Engineering and 2025 IEEE Industrial and Commercial Power Systems Europe (EEEIC / ICPS Europe)*, pages 1–7, 2025.

[29] Grand View Research. Europe virtual power plant market size, share & trend analysis report, 2024. Segment Forecasts, 2025–2030.

[30] Energy Systems Integration Group (ESIG). Der integration into wholesale markets and operations, 2021.

[31] A. Fusco, D. Gioffrè, A. F. Castelli, C. Bovo, and E. Martelli. A multi-stage stochastic programming model for the unit commitment of conventional and virtual power plants bidding in the day-ahead and ancillary services markets. *Applied Energy*, 336:120739, 2023.

[32] Linda Brodnicke, Febin Kachirayil, Paolo Gabrielli, Giovanni Sansavini, and Russell McKenna. Transforming decentralized energy systems: Flexible ev charging and its impact across urbanization degrees. *Applied Energy*, 384:125303, 2025.

[33] Kelsey Nelson, Javad Mohammadi, Yu Chen, Alex Aved, David Ferris, Erik Blasch, Erika Ardiles Cruz, and Philip Morrone. Benefits and vulnerabilities of managing a growing fleet of networked electric vehicles. *IEEE Transactions on Industry Applications*, 61(2):1917–1926, 2025.

[34] Department of Energy Office of Electricity. Impact of electric vehicles on the grid - report to congress. Technical report, 2024.

[35] H. Pakbin, A. Karimi, and M. N. Hassanzadeh. An optimized demand response framework for enhancing power system reliability under wind power and ev-induced uncertainty. *Scientific Reports*, 15:21636, 2025.

[36] Free2move eSolutions S.p.A. Free2move website, 2024.

[37] Terna. Workshop progetti pilota, 2020. 4 dicembre 2020.

[38] ARERA. Annual report 2024 – report to acer and the european commission. Technical report, July 2024.

[39] Ksenia Poplavskaya, Jesus Lago, and Laurens de Vries. Effect of market design on strategic bidding behavior: Model-based analysis of european electricity balancing markets. *Applied Energy*, 270:115130, 2020.

[40] Y. Zhang, J. Han, and Y. Shi. Risk-aware value-oriented net demand forecasting for virtual power plants. *arXiv preprint*, June 2024.

[41] H. Nemati, P. Sánchez-Martín, Á. Ortega, L. Sigrist, E. Lobato, and L. Rouco. Flexible robust optimal bidding of renewable virtual power plants in sequential markets. *arXiv preprint*, February 2024.

[42] e-distribuzione. Il progetto edge, 2025.

[43] Luis Rios and Nikolaos Sahinidis. Derivative-free optimization: A review of algorithms and comparison of software implementations. *Journal of Global Optimization*, 56, 11 2009.

[44] J. A. Nelder and R. Mead. A simplex method for function minimization. *The Computer Journal*, 7(4):308–313, 01 1965.

[45] Varun Chandola, Arindam Banerjee, and Vipin Kumar. Anomaly detection: A survey. *ACM Comput. Surv.*, 41(3), July 2009.

[46] Moritz Weber, Marian Turowski, Hüseyin K. Çakmak, Ralf Mikut, Uwe Kühnapfel, and Veit Hagenmeyer. Data-driven copy-paste imputation for energy time series. *IEEE Transactions on Smart Grid*, 12(6):5409–5419, 2021.

[47] David A. Howe and Chloe Champagne. Time-series imputation algorithm. *IEEE Signal Processing Letters*, 2021.